Nano Res
DOI 10.1007/s12274-011-0118-9
Research Article

ISSN 1998-0124
CN 11-5974/O4

Tunable Separation of Single-Walled Carbon Nanotubes by Dual-Surfactant Density Gradient Ultracentrifugation

Pei Zhao[1], Erik Einarsson[1,2], Georgia Lagoudas[3], Junichiro Shiomi[1], Shohei Chiashi[1], and Shigeo Maruyama[1] (✉)

[1] Department of Mechanical Engineering, The University of Tokyo, Tokyo 113-8656, Japan
[2] Global Center of Excellence for Mechanical Systems Innovation, The University of Tokyo, Tokyo 113-8656, Japan
[3] Department of Bioengineering, Rice University, Houston 77005, USA

Received: 11 January 2011 / Revised: 24 February 2011 / Accepted: 1 March 2011

ABSTRACT

We present a systematic study of the effects of surfactants in the separation of single-walled carbon nanotubes (SWNTs) by density gradient ultracentrifugation (DGU). Through analysis of the buoyant densities, layer positions, and optical absorbance spectra of SWNT separation using the bile salt sodium deoxycholate (DOC) and the anionic salt sodium dodecyl sulfate (SDS), we clarify the roles and interactions of these two surfactants in yielding different DGU outcomes. The separation mechanism described here can also help in designing new DGU experiments by qualitatively predicting outcomes of different starting recipes, improving the efficacy of DGU and simplifying post-DGU fractionation.

KEYWORDS

Single-walled carbon nanotubes, density gradient ultracentrifugation, sodium deoxycholate, sodium dodecyl sulfate

1. Introduction

The one-dimensional structure of single-walled carbon nanotubes (SWNTs) imparts them with a variety of remarkable physical, chemical, and biological properties. Due to these numerous desirable characteristics, SWNTs have potential uses in a wide range of applications including electronics, optics, and biosensors [1]. However, since the electrical nature of an SWNT is structure-dependent, their widespread use in applications will remain limited until homogeneous SWNTs can be obtained in sufficient quantities. Direct synthesis of homogeneous SWNTs is of course the most desirable solution, but this is not yet possible using current production methods. Various post-production separation methods, however, have been developed over the last few years to obtain small amounts of SWNTs with a specific chirality or electronic type [2–20]. Of all these techniques, the density gradient ultracentrifugation (DGU) method, adapted to SWNTs by Arnold et al. [6, 7], is considered one of the most promising and effective for achieving good SWNT selectivity not only by electronic type [7, 11–14] but also diameter [6, 7, 15–20] and even chirality [6, 7, 18–20].

Generally speaking, in the DGU method SWNTs are suspended in water by dispersing with one or more surfactants, which form micelles around the SWNTs. Different wrapping morphologies form micelles of different sizes and densities, and DGU is then used to separate the surfactant-wrapped SWNTs based on these small density differences. While the choice of surfactant and density gradient profile are very

Address correspondence to maruyama@photon.t.u-tokyo.ac.jp

important, with the former playing the most critical role, the role of the surfactant has not been systematically investigated and the relationship between the surfactant and the DGU outcome remains unclear.

In this work we systematically investigate how the two common surfactants sodium deoxycholate (DOC) and sodium dodecyl sulfate (SDS) influence DGU separation of SWNTs. Analysis of the resulting buoyant densities, layer positioning, and optical absorbance spectra show that wrapping by the bile salt DOC is necessary to obtain diameter-dependent separation of SWNTs, while wrapping by the anionic salt SDS leads to separation by electronic type. Critically, however, the surfactant environment during DGU can significantly affect the final outcome, which we explain by considering surfactant concentrations and exchange processes. By considering the surfactant roles and interactions presented here, one can more effectively design DGU recipes tailored to achieve a desired final separation and to simplify post-DGU fractionation in order to extract high purity samples.

2. Experimental

The SWNTs used in these experiments were synthesized by the alcohol catalytic chemical vapor deposition (ACCVD) method [21]. These SWNTs more effectively reveal the efficacy of the DGU process due to their broader diameter distribution than that of CoMoCAT SWNTs. Furthermore, ACCVD SWNTs tend to have a narrower chirality distribution [22] than HiPco SWNTs, thus are more easily analyzed. However, our results are not limited to ACCVD SWNTs [19] and essentially the same results were obtained using HiPco SWNTs as shown in Fig. S-1 in the Electronic Supplementary Material (ESM).

SWNTs were dispersed in DOC and/or SDS by ultrasonication for 30 min at 400 W/cm^2 using a horn-type ultrasonicator (UP-400S, Hielscher Ultrasonics). The dispersion was then immediately centrifuged at 276,000 g for 15 min while maintained at a temperature of 22 °C, and the upper 80% of the supernatant was carefully decanted. In Case I, this decanted supernatant was diluted by iodixanol stock (OptiPrep™ density gradient medium, Sigma–Aldrich Co., Ltd.) to a sample layer with 30% iodixanol, while in Case II it was directly used as the sample layer. A density gradient column was formed separately inside a 5 mL polycarbonate centrifuge tube (approx. 1.3 cm diameter, 5.2 cm in length) by layering different concentrations of iodixanol–water solutions. The two density gradient profiles used in our DGU experiments are as follows: in Case I the profile contained 1 mL each of 20%, 30%, and 40% v/v iodixanol in D_2O, whereas in Case II it contained 0.4 mL of 20%, 1 mL of 30%, 1 mL of 40%, and 0.6 mL of 60% v/v iodixanol in D_2O. In some experiments, DOC and/or SDS were also introduced into the density gradient medium at different concentrations (see the Experimental section in the ESM). After layering, the density gradient column was placed horizontally and allowed to diffuse for 1 h in order to create a smooth density gradient profile. The sample layer of the SWNT dispersion was then carefully injected at a point where its density approximately matched that of the density gradient (Case I) or placed on top of the density gradient (Case II). The columns were then ultracentrifuged at 197,000 g using a Hitachi Koki S52ST swinging bucket rotor. After centrifugation, each of the resulting layers was extracted and collected using a micropipette (details of the SWNT separation are given in the ESM). Ultra violet–visible–near infrared (UV–Vis–NIR) absorbance spectra (UV-3150 spectrometer, Shimadzu) and photoluminescence excitation spectra [23] (HORIBA Jobin Yvon Fluorolog iHR320, equipped with a liquid-nitrogen-cooled GaAs detector) of the fractionated samples were then measured and analyzed.

3. Results

3.1 Case I: Insignificant change in surfactant environment

The detailed procedure for Case I is shown in Fig. 1(a), where we initially dispersed SWNTs in DOC and/or SDS and then injected them into the density gradient medium so that their initial position was approximately the same as their final position in the column. Since this results in minimal movement of SWNTs through the DGU column, changes in the surfactant environment around the SWNTs are negligible.

It has been demonstrated that initial dispersion of

SWNTs in DOC followed by DGU in a density gradient medium containing SDS results in diameter-dependent separation of SWNTs [19, 20]. We further investigated the role of SDS by introducing it at different stages during the DGU process and in different concentrations. We refer to SDS used for the initial dispersion of SWNTs as SDS-I, and SDS included in the density gradient column as SDS-II. Figure 1(b) shows the concentrations of co-surfactants in a series of systematic trials, and the corresponding DGU results are shown in Fig. 1(c).

In Trial 1 the SWNTs were initially dispersed in DOC but both SDS-I and SDS-II were absent during DGU. This resulted in no separation of SWNTs. Essentially the same result was obtained in Trial 2, where only DOC and SDS-I were used. A similar result was obtained in Trial 8, where both SDS-I and SDS-II were present but DOC was absent. We note that this condition (Trial 8) is known to result in separation by electronic type [13], but as shown later requires a steeper density gradient if it is to be observed. All other trials (Trials 3–7) resulted in different degrees of diameter-dependent separation of SWNTs. This clearly demonstrates that in order to achieve diameter-dependent separation of SWNTs, DOC must be present during the dispersing step and SDS must be present during DGU (i.e., the SDS-II concentration must be non-zero).

The influence of SDS-I was investigated by changing the concentration of SDS-I while maintaining a constant concentration of SDS-II (1.5% *w*/*v*; *w*/*v* means the mass of surfactant in the density gradient medium/volume

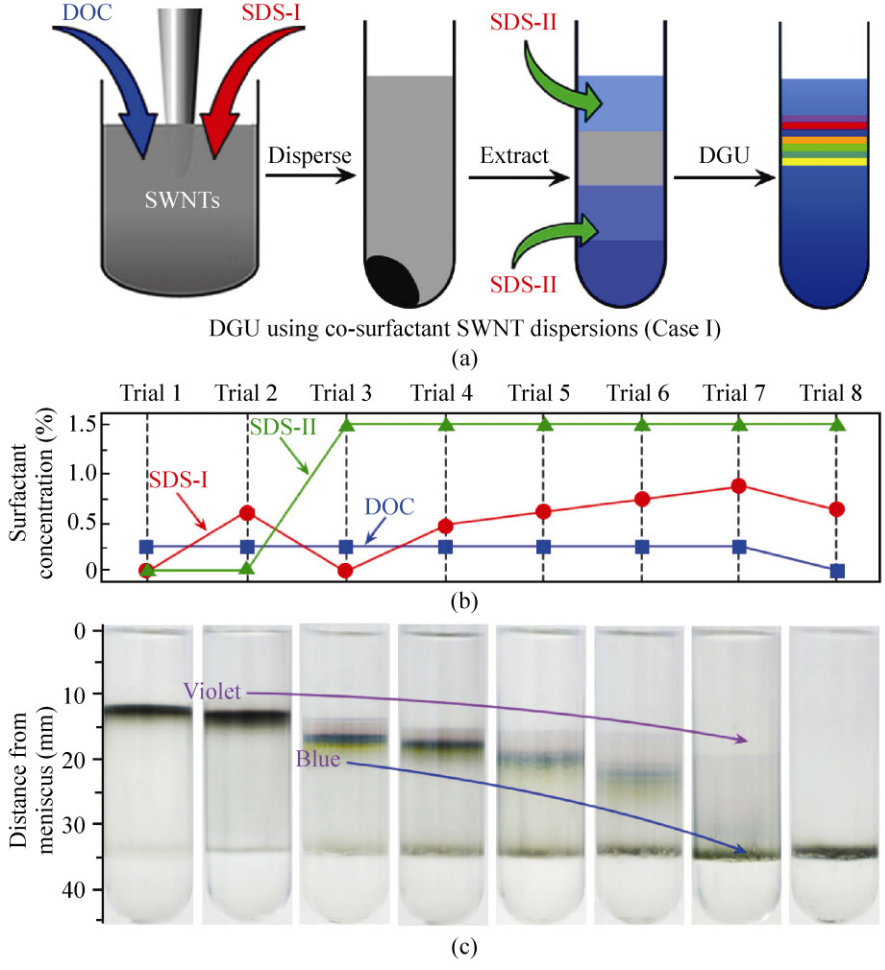

Figure 1 Density gradient ultracentrifugation results using co-surfactant SWNT dispersions for Case I. (a) Experimental procedure; see text for definitions of SDS-I and SDS-II. (b) Co-surfactant recipes for the realization and expansion of the separated region using DOC and SDS. (c) Corresponding experimental results obtained for Trials 1–8

of the medium) and DOC (0.5% *w*/*v*). These experiments correspond to Trials 3–7, and the outcomes are shown in Fig. 1(c). All of these trials resulted in diameter-dependent separation, but increasing the concentration of SDS-I from 0% (SWNTs initially dispersed only by DOC) to 0.875% *w*/*v* increasingly broadened the final separated region. In addition to this broadening, the position of each layer also shifted downward with increasing SDS-I concentration, indicating an overall increase in the density of the surfactant–SWNT micelles. Note that the lower layers shift more than the upper layers, and the highest concentrations of SDS-I (Trial 7 in Fig. 1(c)) increased the density of the surfactant–SWNT micelles to such an extent that some of the larger diameter nanotubes (in the green and yellow layers) sank down to the bottom of the density gradient column.

Broadening of the diameter-dependent separated region observed for Trials 3–7 in Fig. 1(c) can also be realized by introducing SDS-I during an intermediate stage, as shown by the process in Fig. 2(a). In these experiments, SWNTs were initially dispersed using only DOC, and the supernatant was extracted after ultracentrifugation. SDS-I was then added to the DOC-dispersed SWNTs, and the mixture was injected into the density gradient profile as previously described. The concentrations used are shown in Fig. 2(b). This approach also resulted in diameter-dependent separation, with similar SDS-I concentrations (compared to the process shown in Fig. 1(a)) resulting in similar separations. However, the effect of the SDS-I concentration on the expansion of the separated region was different: as shown in Fig. 2(c), some of the layers

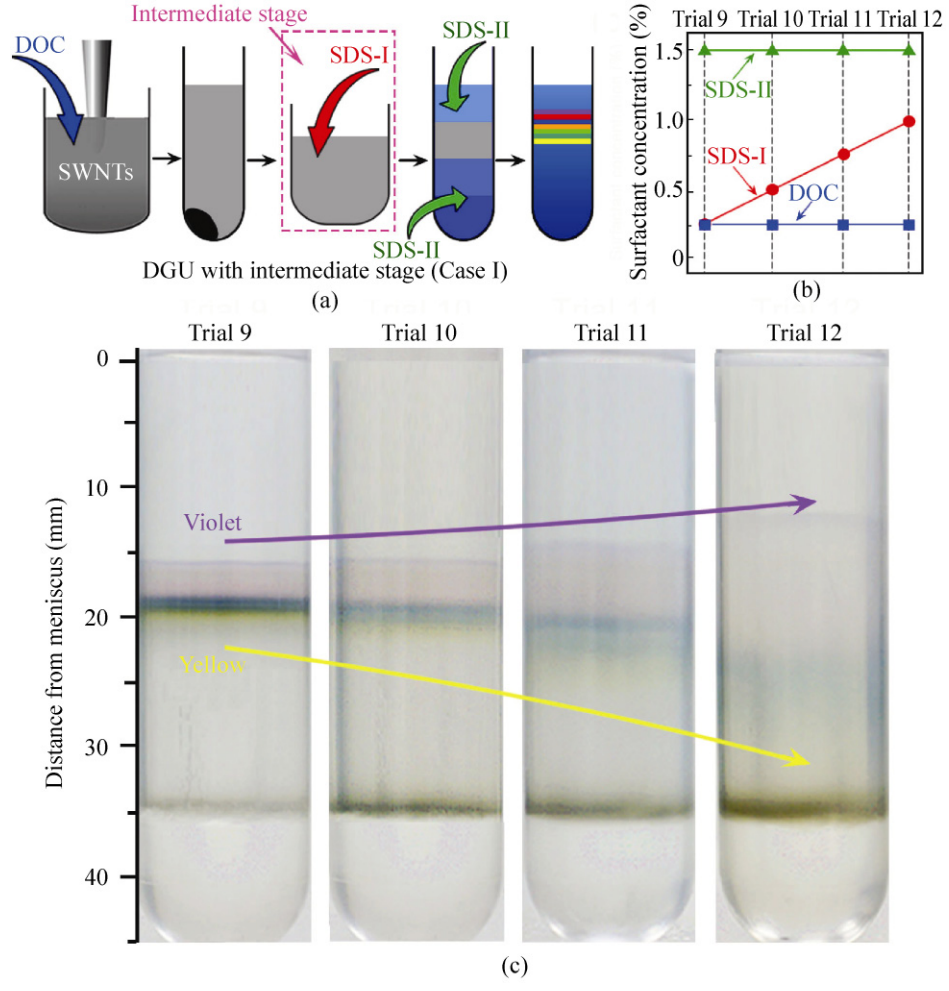

Figure 2 (a) DGU experimental procedure using an intermediate stage for Case I. (b) Co-surfactant recipes for expansion of the separated region. (c) Corresponding experimental results obtained for Trials 9–12

moved upward with increasing SDS-I concentration and the reason for this will be discussed later.

3.2 Case II: Changing surfactant environment

To further investigate the role of surfactants during DGU we adopted a second approach, as shown in Fig. 3(a). In this approach, SWNTs were dispersed in a mixture of DOC and SDS, and then placed on top of the density gradient column. As a result, the SWNT micelles were forced to move down through the density gradient column during DGU in order to reach their isopycnic points. Contrary to Case I, this leads to significant changes in the surfactant environment. Using this approach a steeper density gradient profile was necessary to obtain the final separation, so we used a nonlinear density gradient column in Case II (as described in the Experimental section). As in Case I, the following results can be essentially duplicated by introducing SDS-I during an intermediate stage instead of during the initial dispersion. This is shown in Fig. S-2 in the ESM.

Starting with the same DOC–SWNT dispersion as in Case I (SWNTs dispersed in DOC) and gradually increasing the concentration of SDS-I to form a co-surfactant dispersion, we obtained different but related results. Surfactant concentrations are shown in Fig. 3(b). The photograph in Fig. 3(c) is representative of the resulting separations, in which we find two very different bands of SWNTs. When SWNTs were only dispersed in DOC (0% SDS-I), the thickness of this upper band was approximately 1 mm and appeared to contain three different colored layers (Trial 13). Optical absorbance spectra obtained from these bands (Fig. 4) revealed that this band consisted of small-diameter near-armchair nanotubes. A weak trend of increasing diameter was evident in the successive colored layers,

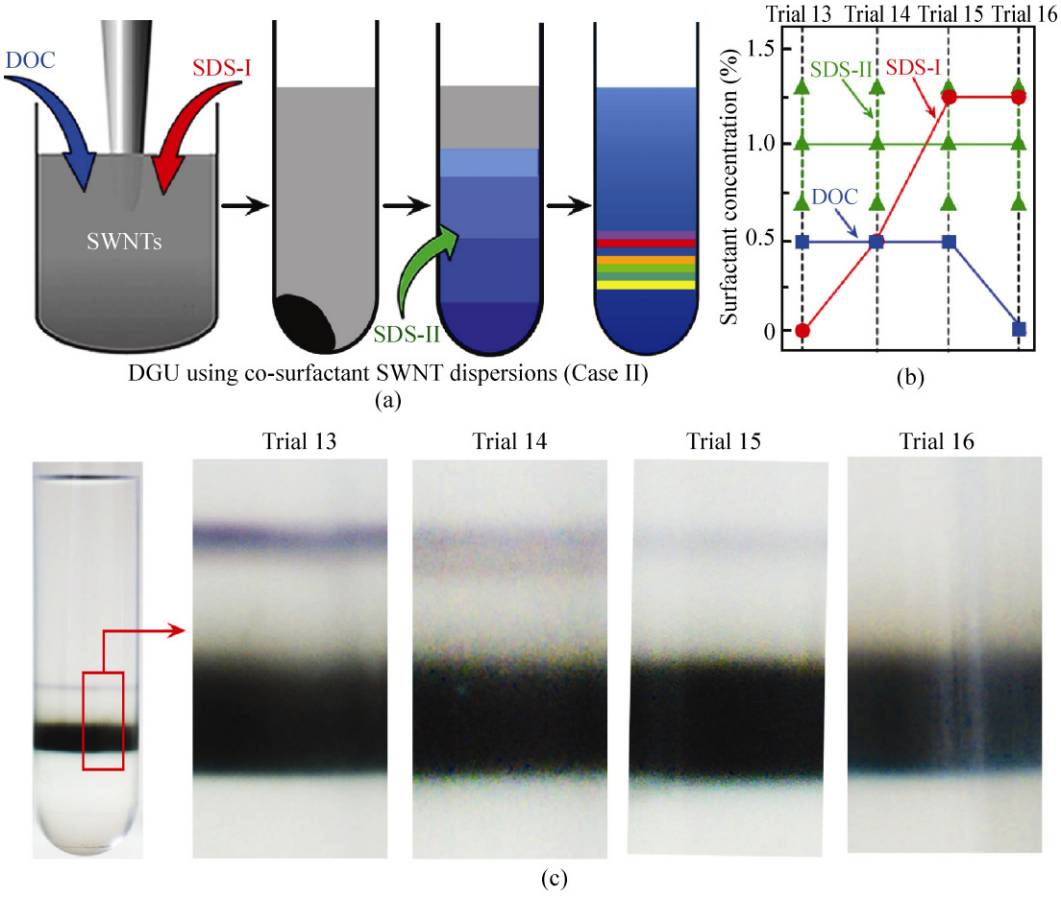

Figure 3 Density gradient ultracentrifugation results for Case II. (a) Experimental procedure. (b) Co-surfactant recipes of the separation in Trials 13–16. For each trial, the three green triangles indicate the concentration of SDS-II in the 40%, 30%, and 20% layers. (c) Corresponding experimental results of Trials 13–16

reminiscent of the results obtained in Trials 3–7 in Case I. When 0.5% *w*/*v* SDS-I was included during dispersion (Trial 14), the number of visible colored layers contained in this upper band decreased to only two, violet, and red. The violet layer was highly enriched in (6,5) nanotubes, while the red layer contained primarily (6,5) and (7,5) nanotubes. These colors and corresponding (*n*,*m*) species are the same as those found for diameter-dependent separation of SWNTs in our previous report [19]. Increasing the SDS-I concentration to 1.25% *w*/*v* (Trial 15) resulted in more effective isolation of (6,5) nanotubes in this upper separation band and the disappearance of the red layer. Finally, when the SWNTs were dispersed only in SDS (0% DOC), no upper band was observed (Trial 16). This confirms the isolation of small-diameter SWNTs found in this upper band is due to wrapping by DOC.

Approximately 4 mm below the thin upper band was a wide, dark band of what appeared to be an unsorted collection of SWNTs. Careful inspection, however, revealed regions of blue and dark yellow extending below and above the unsorted region (see Fig. 3(c)). Optical absorbance spectra obtained from these regions (shown in Fig. 4) indicated that the dark yellow region consists primarily of metallic SWNTs, while the bluish region contained primarily semiconducting SWNTs. This electronic-type separation is not as efficient as that previously reported by other groups [11–13], and thus the diameter distribution in these regions cannot be accurately determined. The role of SDS, however, can be understood from Trial 16, in which DOC was absent and the SWNTs were initially dispersed only by SDS. This procedure resulted in no upper separation band, but electronic-type separation was achieved in the lower band. Since only SDS was involved during this entire process, the SWNT–micelles can only be composed of SDS at all stages of separation. This separation of metallic and semiconducting SWNTs suggests that the SDS micelles change considerably during DGU, with the final micelles becoming significantly denser than in the initial dispersion. The micelle structure must also be dependent on the electronic nature of the nanotube.

The time-dependent evolution of Trial 15 is shown in Fig. 5. This was performed using a co-surfactant SWNT dispersion containing 0.5% *w*/*v* DOC and 1.25% *w*/*v* SDS, and was evaluated every two hours. The distribution ranges of the violet, dark yellow, and blue components are indicated by vertical bars, and the positions of highest apparent concentration (i.e., richest color) are connected by a line. These data were obtained from the absorbance spectra shown in Fig. S-3 in the ESM. Emergence of the violet (6,5) layer from the pristine material was found to occur very quickly, beginning to appear after only one hour of DGU. After 9 h, the violet layer reached its isopycnic point and

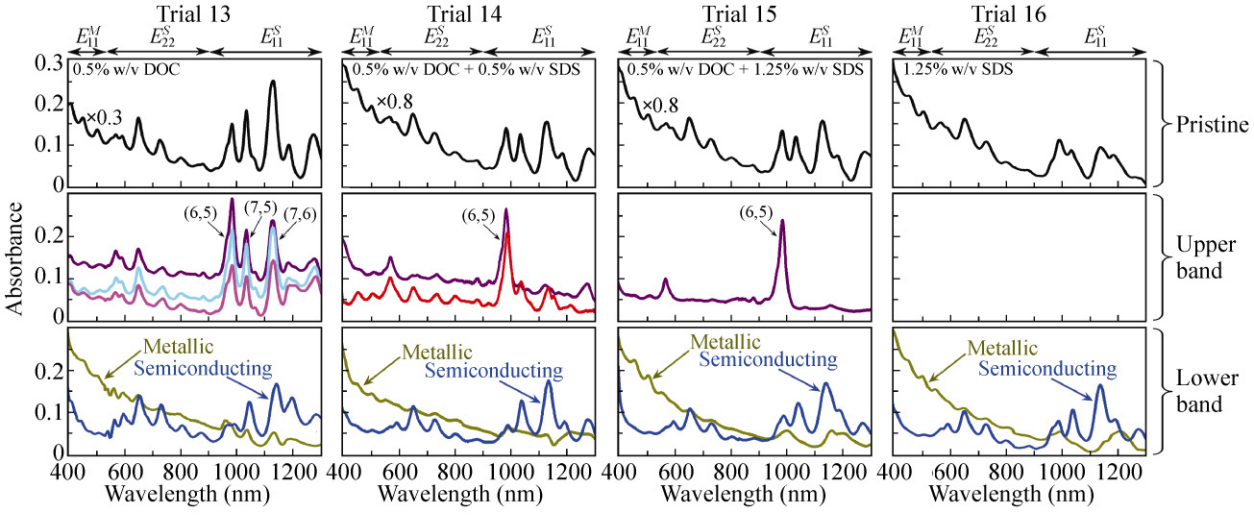

Figure 4 Optical absorption spectra of each separated layer in both upper and lower bands of Trials 13–16, absorbance spectra of the pristine materials are shown at top for reference. The colors of layers are labeled using the colors they appear to the eye

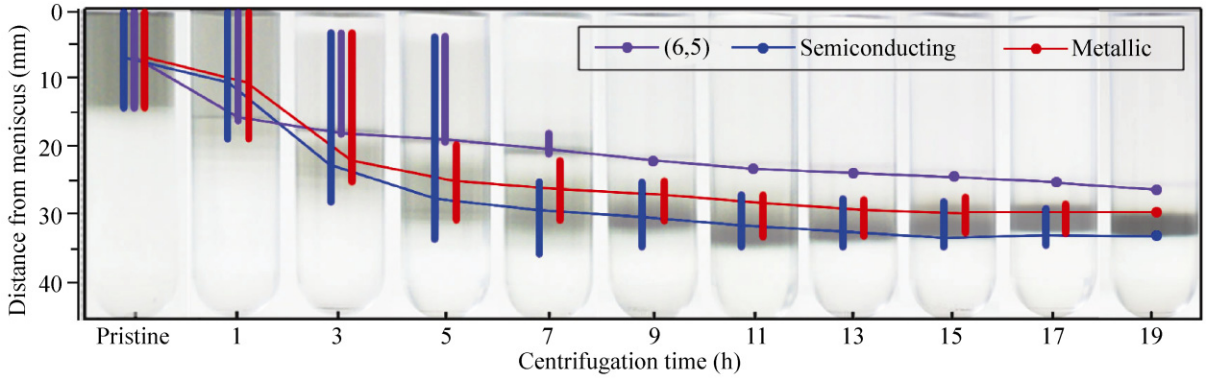

Figure 5 Time-dependent evolution of DGU separation starting with SDS/DOC co-surfactant dispersed SWNTs (Trial 15). The traces of the three primary separated components, violet, metallic, and semiconducting layers, are marked as a function of time. The bar indicates the apparent spread of the band, and the line connects the positions at which the band appears most concentrated

its shape did not change any further. Separation by electronic type, however, required at least 15 h to observe even slight changes indicating metallic and semiconducting enriched regions, respectively above and below the blackish, unseparated region.

4. Discussion

4.1 Roles of the surfactants

Firstly we note that although our trials were performed using a D_2O/H_2O system (OptiPrep™ density gradient medium is a commercial dilution of iodixanol by H_2O), the final results are essentially the same as for a pure H_2O system (see Fig. S-4 in the ESM) During the DGU process, replacement of hydrated D_2O and H_2O molecules in SWNT–micelles can result in some different diffusion processes; however, this can be ignored because we systematically changed only the surfactant concentration in all trials. Therefore, in the following discussion we only focus on the influence of the surfactants on the DGU results.

Comparison of SWNT separations obtained by single-surfactant DGU performed using identical density gradient profiles reveals that SDS-wrapped SWNTs have higher densities than DOC-wrapped SWNTs (see Fig. S-5 in the ESM). This is attributed to the considerable hydration layer that accompanies DOC [24, 25], which increases the micelle volume of DOC-wrapped SWNTs. For the dual-surfactant case, we have hypothesized that the structure of surfactant-dispersed SWNTs is a DOC-wrapped SWNT with SDS molecules loaded onto the available space between DOC molecules [19]. Since hydrated SDS molecules are considerably smaller than hydrated DOC molecules, SDS loading increases the mass of the micelles while having a minimal effect on the volume. Additionally, since the DOC packing density decreases with increasing SWNT diameter there is more space available for SDS adsorption on larger diameter SWNTs [20]. This explains why diameter-dependent separation (e.g., Trials 3–7) sorts the SWNTs such that larger diameter SWNTs are found in the higher density regions of the DGU column. Increasing the concentration of SDS in the column (SDS-II) increases its loading onto the SWNTs, resulting in an enhancement of the initially small buoyant density differences for SWNTs of different diameter (Trials 3–7). The increase in SDS-II concentration can also alter the composition of the micelles, but the extent of the changes depends primarily on the relative affinities between the surfactants and the SWNTs.

Due to its somewhat planar structure, DOC is thought to have a stronger affinity for SWNTs than the linear SDS, and may interact more strongly with nanotubes of certain chiralities [7, 15–20]. Because of this high affinity, DOC-wrapped small-diameter SWNTs are stable even in environments containing high concentrations of SDS. However, the affinity for DOC weakens considerably as the SWNT diameter increases. This can be seen from the optical absorption spectra of the pristine material, as shown in Fig. 4.

Dispersion of SWNTs using different surfactant recipes leads to different surfactant concentrations, and an increase in SDS concentration will decrease the absorbance from large-diameter nanotubes. Therefore we assume that SDS can replace DOC molecules on large-diameter nanotubes more easily than on nanotubes with smaller diameters. This reduces the hydrated volume of the surfactant–SWNT micelles, increasing the buoyant densities of larger diameter nanotubes. This is the reason for the downward shift seen in Fig. 1(c) that is dependent on SDS concentration. If SDS is introduced immediately prior to DGU, as in Fig. 2(a), the SWNTs are surrounded by both DOC and SDS with the same concentrations during the entire DGU process. The equilibrium state in both cases (with or without an intermediate stage) will be the same, which is why the final results are similar in both cases. However, trials with an intermediate stage require different times to reach the equilibrium state than trials in which SWNTs are initially dispersed simultaneously by DOC and SDS. This time is shorter for small-diameter nanotubes wrapped only by DOC. Considering the diffusion of the density gradient medium, this causes some of the small-diameter nanotubes wrapped by DOC to shift upward instead of downward.

The results obtained for Case I, and for related experiments, can be explained by considering the surfactant–SWNT micelles. Addition of SDS to the density gradient medium (SDS-II) will serve to either replace DOC with SDS or to attach more SDS to the pre-existing DOC-wrapped SWNTs. The final micelle composition and morphology are determined by the initial concentrations of DOC and SDS-I, the concentration of SDS-II, the relative affinities between the SWNTs and surfactants present in the local environment, as well as the dynamic equilibrium between the surfactants adsorbed onto the nanotubes and free surfactant molecules present in the surrounding environment [26–28]. For Case II, however, the changing surfactant environment adds another level of complexity to the overall process.

4.2 Importance of the surfactant environment

Density profiles for Case I and Case II, along with initial and final positions of the SWNTs, are shown in Fig. 6. For Case I, the final separation is found in the same region as that where the dispersion was initially injected (see the Experimental section). Moreover, free DOC and SDS molecules in the initial dispersions, as well as SDS molecules contained in this region of the density gradient column, are always available to the SWNT micelles. In Case II, on the other hand, the SWNT dispersion is placed on top of the density gradient column, forcing the SWNTs to move down through the density gradient column during DGU. This causes the SWNTs to move from a DOC-rich environment into an SDS-rich environment, significantly affecting the morphology and composition of the surfactant–SWNT micelles. This is especially clear when the pristine dispersion contains much more SDS than DOC. This leads to easier replacement of DOC

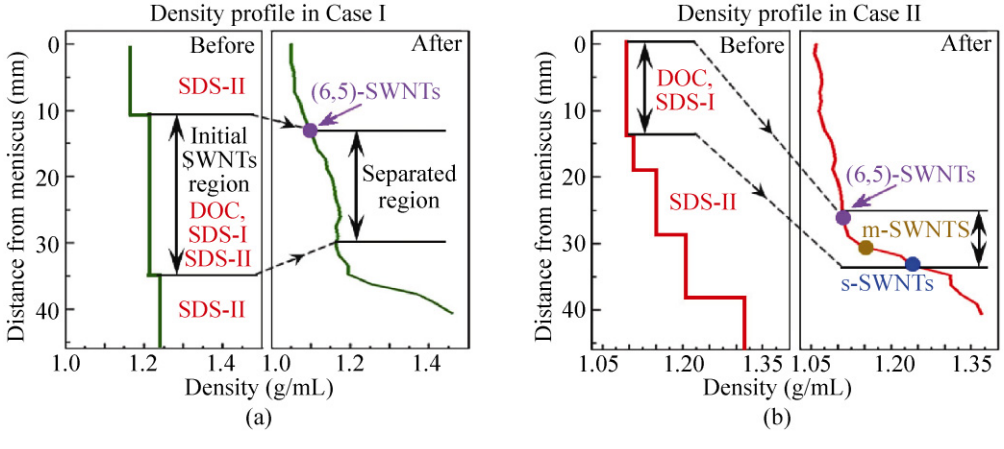

Figure 6 Density profiles (a) in Case I and (b) in Case II before and after the DGU process. Initial dispersion and post-DGU regions are indicated

by SDS when moving through the SDS-containing density gradient medium. The result is separation of metallic and semiconducting nanotubes, as well as simultaneous isolation of small-diameter near-armchair nanotubes (Trials 13–15).

To understand the outcomes in Case II, we analyzed the buoyant densities of (6,5) nanotubes found in the violet layers obtained in various trials for both Cases. Prior to DGU, the densities of the co-surfactant SWNT micelles in all the initial dispersions were found to be approximately 1.1 g/mL, which is similar to that of the D_2O used as the dispersing medium. After DGU, the densities of the violet layers ranged from approximately 1.11 g/mL to 1.15 g/mL, as determined from the positions in the density gradient profile shown for Case I in Fig. 6(a). For Case II, the violet layers found in the upper bands in Trials 13, 14, and 15 were also found to have buoyant densities of approximately 1.11 g/mL. The final densities of the lower bands, however, were approximately 1.13 g/mL for metallic SWNTs and 1.23 g/mL for semiconducting SWNTs, including a small population of (6,5) nanotubes contained in this layer. This indicates significant changes in the composition and morphology of the surfactant–SWNT micelles in Case II. Evidence of these changes can also be found in the absorbance spectra obtained from the various trials.

An absorbance spectrum of pre-DGU, DOC-dispersed SWNTs is shown in Fig. 7, and the positions of the dominant peaks for Trials 13, 15, and 16 in Case II are indicated in the upper portion of the figure. If we focus on the E_{11} absorbance feature of (6,5) SWNTs, we find this peak is located at 983 nm when dispersed only by DOC, and is located at 976 nm when dispersed only by SDS. Interestingly, when dispersed by 0.5% *w/v* DOC and 1.25% *w/v* SDS, the (6,5) E_{11} peak is found at the same location as when dispersed only in DOC, i.e., at 983 nm. The peak position is essentially unchanged for the (6,5) SWNTs constituting the violet layers found in Trials 13–15, as well as for the trials in Case I (not shown). There are, however, weak (6,5) signals detected in the blue semiconducting-rich regions found near the bottom of the DGU columns of Trials 13–16. The position of this peak was between 989 and 994 nm, indicating a considerable change in micelle composition as the SWNT micelle moved down

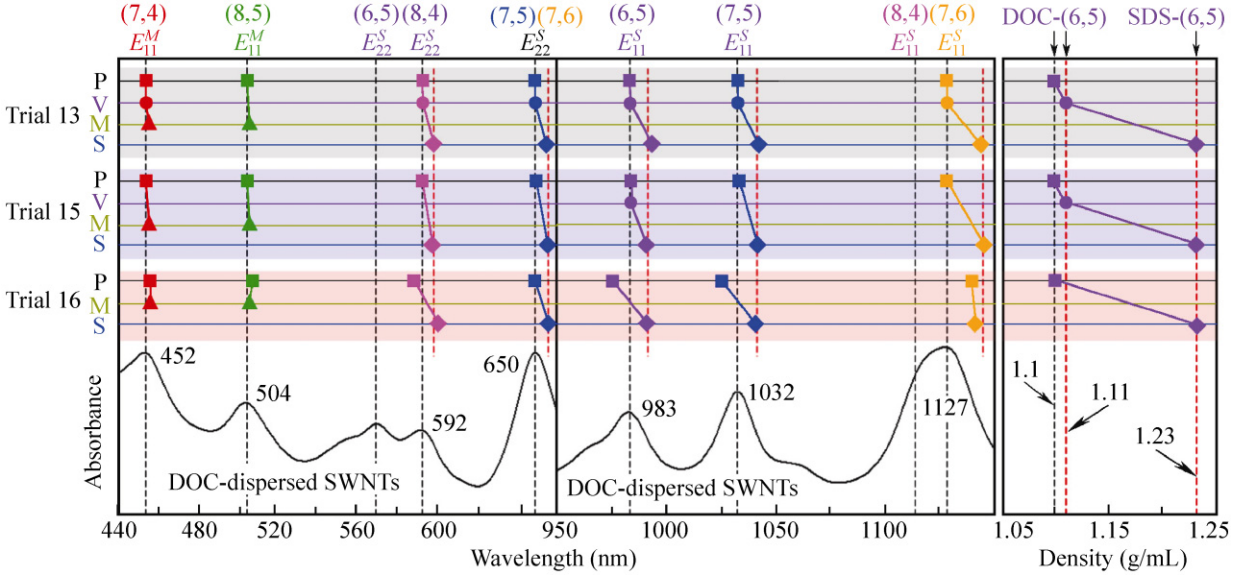

Figure 7 Optical absorption peak positions for several metallic and semiconducting chiralities and dispersion densities (right). The absorbance spectrum of DOC-dispersed SWNTs is shown at the bottom for reference. Background colors of gray, blue, and red indicate Trials 13, 15, and 16, respectively, and horizontal lines of different colors indicate different separated layers, as indicated on the left axis (P: pristine, V: violet, M: metallic, S: semiconducting). Average densities of (6,5) nanotubes enriched in different separated layers are shown on the right. Their different densities suggest different micelle compositions. Vertical red dashed lines indicate shifted positions of those data. Redshifts from (8,4) E_{11} and (6,5) E_{22} are not shown because of their low intensities, and the redshift of the peak at 650 nm indicates a combined shift of both (7,5) E_{22} and (7,6) E_{22}

through the density gradient medium.

To further investigate this composition change during DGU, we measured the (7,5) E_{11} peak position from different DGU fractions extracted every two hours. These data, which are plotted in Fig. 8, are from optical absorbance spectra obtained during the time-dependent analysis of Trial 15 (see Fig. 5). In pristine co-surfactant SWNT dispersions (0.5% *w*/*v* DOC and 1.25% *w*/*v* SDS), the E_{11} position for (7,5) SWNTs is located at 1033 nm, which is essentially the same position as for pure DOC–SWNT dispersions (E_{11} = 1032 nm). During DGU, however, the peak position redshifts as the nanotubes move down through the column into a more SDS-rich region, and the final E_{11} peak position of (7,5) SWNTs located in the lower semiconducting band is at 1042 nm. This redshift during the evolution of the DGU process confirms the change in the composition of surfactant–SWNT micelles results from the changing surfactant environment.

4.3 Summary of the separation mechanism

The results presented in this report cannot be explained in a consistent fashion without considering the dynamic surfactant environment. As discussed above, SDS can gradually replace DOC, with the extent of this exchange being determined by their relative affinities to the SWNTs. The affinities are diameter-dependent, and any surfactant addition or exchange alters the micelle composition. Near-complete replacement of DOC by SDS results in separation of SWNTs by electronic type in the high-density region of the DGU column, which is essentially the same result as obtained when DOC is absent (Trial 16). The mechanism driving this separation has been explained by differences in the electronic structures of metallic and semiconducting SWNTs, which results in a higher loading of SDS onto the metallic nanotubes [13]. Our findings do not contradict the proposed mechanism, and clearly show that SDS is required for electronic-type separation.

For small-diameter near-armchair nanotubes, the DOC–SWNT structure remains stable even in the SDS environment. This is because the affinity with DOC is strong enough to prevent replacement by SDS. This DOC-wrapping leads to the diameter-dependent separation observed in the upper region of Trials 13–15, in which the densities of the small SWNT micelles are almost the same as in the diameter-dependent expansions observed in Case I. A cartoon representation of the surfactant-SWNT micelles in different surfactant environments is presented in Fig. 9.

5. Conclusion

We have shown a continuous enhancement of DGU separation of SWNTs by using dual-surfactant DGU recipes using DOC and SDS. Our findings provide a clearer understanding of the surfactant–SWNT interactions that govern the outcomes of DGU. This knowledge can help in designing DGU recipes such that desired results can be obtained with greater success. Moreover, by enhancing the DGU outcomes our results can also simplify the post-DGU fractionating

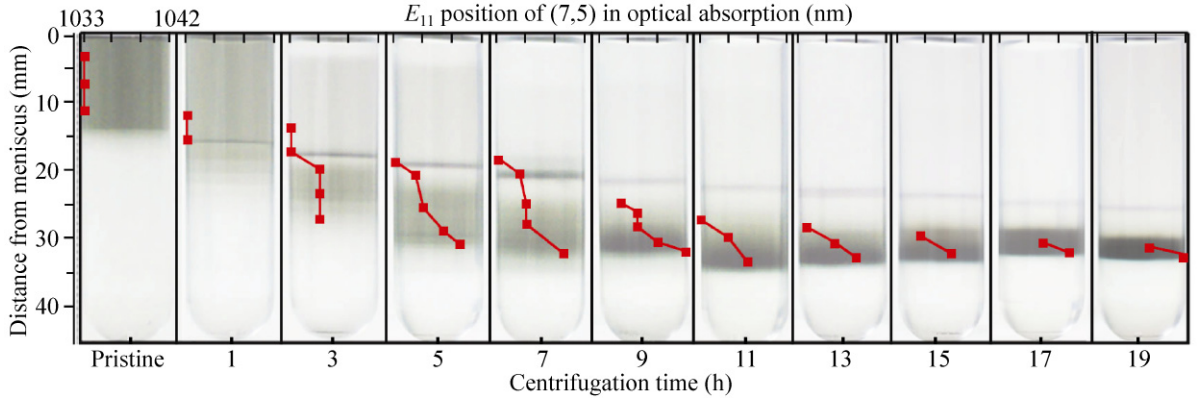

Figure 8 E_{11} position of (7,5) nanotubes in Trial 15 during time-dependent separation in Case II. All ten columns have the same wavelength unit for the upper axis (from 1033 to 1042 nm) as shown in the pristine column

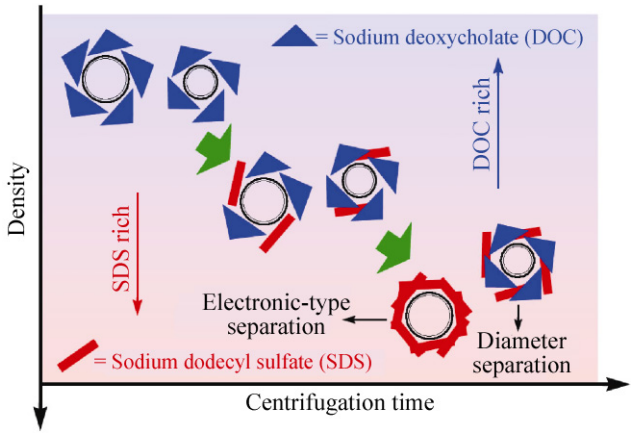

Figure 9 Wrapping structures of different nanotubes under different co-surfactant environments

procedure, which remains one of the most difficult aspects of obtaining well-separated SWNTs by DGU. Although our experiments were conducted using DOC and SDS co-surfactants, we believe our conclusions should be applicable to bile salts and anionic salts in general, as their interactions with SWNTs are dependent on their general structures. Based on the roles of the surfactants clarified by this study, the efficacy of the DGU technique can be significantly improved by considering the various parameters, such as the type and amount of surfactants, buoyant densities of SWNT micelles, and the density gradient profile.

Acknowledgements

Part of this work was financially supported by Grant-in-Aid for Scientific Research (No. 22226006 and 19054003), "Development of Nanoelectronic Device Technology" of New Energy and Industrial Technology Development Organization (NEDO), and the Global Centers of Excellence (COE) Program "Global Center for Excellence for Mechanical Systems Innovation". P. Z. acknowledges a scholarship granted by the China Scholarship Council, and G. L. acknowledges support from the NanoJapan program funded by the National Science Foundation.

Electronic Supplementary Material: Supplementary material (experimental details and supplementary figures) is available in the online version of this article at http://dx.doi.org/10.1007/s12274-011-0118-9.

References

[1] Jorio, A.; Dresselhaus, G.; Dresselhaus, M. S. *Carbon Nanotubes: Advanced Topics in the Synthesis, Structure, Properties and Applications (Topics in Applied Physics)*; Springer: Berlin, 2008.

[2] Usrey, M. L.; Lippmann, E. S.; Strano, M. S. Evidence for a two-step mechanism in electronically selective single-walled carbon nanotube reactions. *J. Am. Chem. Soc.* **2005**, *127*, 16129–16135.

[3] Krupke, R.; Hennrich, F.; Löhneysen, H. v.; Kappes, M. M. Separation of metallic from semiconducting single-walled carbon nanotubes. *Science* **2003**, *301*, 344–347.

[4] Banerjee, S.; Hemraj-Benny, T.; Wong, S. S. Covalent surface chemistry of single-walled carbon nanotubes. *Adv. Mater.* **2005**, *17*, 17–29.

[5] Chen, Z.; Du, X.; Du, M.; Rancken, C. D.; Cheng, H.; Rinzler, A. G. Bulk separative enrichment in metallic or semiconducting single-walled carbon nanotubes. *Nano Lett.* **2003**, *3*, 1245–1249.

[6] Arnold, M. S.; Stupp, S. I.; Hersam, M. C. Enrichment of single-walled carbon nanotubes by diameter in density gradients. *Nano Lett.* **2005**, *5*, 713–718.

[7] Arnold, M. S.; Green, A. A.; Hulvat, J. F.; Stupp, S. I.; Hersam, M. C. Sorting carbon nanotubes by electronic structure using density differentiation. *Nat. Nanotechnol.* **2006**, *1*, 60–65.

[8] Zheng, M.; Jagota, A.; Strano, M. S.; Santos, A. P.; Barone, P.; Chou, S. G.; Diner, B. A.; Dresselhaus, M. S.; McLean, R. S.; Onoa, G. B.; Samsonidze, G. G.; Semke, E. D.; Usrey, M.; Walls, D. J. Structure-based carbon nanotube sorting by sequence-dependent DNA assembly. *Science* **2003**, *302*, 1545–1548.

[9] Ju, S. Y.; Doll, J.; Sharma, I.; Papadimitrakopoulos, F. Selection of carbon nanotubes with specific chiralities using helical assemblies of flavin mononucleotide. *Nat. Nanotechnol.* **2008**, *3*, 356–362.

[10] Nish, A.; Hwang, J. Y.; Doig, J.; Nicolas, R. J. Highly selective dispersion of single-walled carbon nanotubes using aromatic polymers. *Nat. Nanotechnol.* **2007**, *2*, 640–646.

[11] Green, A. A.; Hersam, M. C. Colored semitransparent conductive coatings consisting of monodisperse metallic single-walled carbon nanotubes. *Nano Lett.* **2008**, *8*, 1417–1422.

[12] Yanagi, K.; Miyata, Y.; Kataura, H. Optical and conductive characteristics of metallic single-wall carbon nanotubes with

three basic colors; cyan, magenta, and yellow. *Appl. Phys. Express* **2008**, *1*, 034003.

[13] Niyogi, S.; Densmore C. G.; Doorn, S. K. Electrolyte tuning of surfactant interfacial behavior for enhanced density-based separations of single-walled carbon nanotubes. *J. Am. Chem. Soc.* **2009**, *131*, 1144–1153.

[14] Chernov, A. I.; Obraztsova, E. D. Metallic single-wall carbon nanotubes separated by density gradient ultracentrifugation. *Phys. Status Solidi B* **2009**, *246*, 2477–2481.

[15] Hennrich, F.; Arnold, K.; Lebedkin, S.; Quintillá, A.; Wenzel, W.; Kappes, M. M. Diameter sorting of carbon nanotubes by gradient centrifugation: Role of endohedral water. *Phys. Status Solidi B* **2007**, *244*, 3896–3900.

[16] Wei, L.; Lee, C. W.; Li, L. J.; Sudibya, H. G.; Wang, B.; Chen, L. Q.; Chen, P.; Yang, Y.; Chan-Park, M. B.; Chen, Y. Assessment of (*n*,*m*) selectively enriched small diameter single-walled carbon nanotubes by density differentiation from cobalt-incorporated MCM-41 for macroelectronics. *Chem. Mater.* **2008**, *20*, 7417–7424.

[17] Fleurier, R.; Lauret, J. S.; Flahaut, E.; Loiseau, A. Sorting and transmission electron microscopy analysis of single or double wall carbon nanotubes. *Phys. Status Solidi B* **2009**, *246*, 2675–2678.

[18] Green, A. A.; Duch, M. C.; Hersam, M. C. Isolation of single-walled carbon nanotube enantiomers by density differentiation. *Nano Res.* **2009**, *2*, 69–77.

[19] Zhao, P.; Einarsson, E.; Xiang, R.; Murakami, Y.; Maruyama, S. Controllable expansion of single-walled carbon nanotube dispersions using density gradient ultracentrifugation. *J. Phys. Chem. C* **2010**, *114,* 4831–4834.

[20] Ghosh, S.; Bachilo, S. M.; Weisman, R. B. Advanced sorting of single-walled carbon nanotubes by nonlinear density gradient ultracentrifugation. *Nat. Nanotechnol.* **2010**, *5,* 443–450.

[21] Maruyama, S.; Kojima, R.; Miyauchi, Y.; Chiashi, S.; Kohno, M. Low-temperature synthesis of high-purity single-walled carbon nanotubes from alcohol. *Chem. Phys. Lett.* **2002**, *360*, 229–234.

[22] Miyauchi, Y.; Chiashi, S.; Murakami, Y.; Hayashida, Y.; Maruyama, S. Fluorescence spectroscopy of single-walled carbon nanotubes synthesized from alcohol. *Chem. Phys. Lett.* **2004**, *387*, 198–203.

[23] Bachilo, S. M.; Strano, M. S.; Kittrell, C.; Hauge, R. H.; Smalley, R. E.; Weisman, R. B. Structure-assigned optical spectra of single-walled carbon nanotubes. *Science* **2002**, *298*, 2361–2366.

[24] Fontell, K. Micellar behaviour in solutions of bile-acid salts I: Vapor pressure of the aqueous solutions and the osmotic activity of the bile-acid salts. *Kolloid Z. Z. Polym.* **1971**, *244*, 246–252.

[25] Mukerjee, P. The hydration of micelles of association colloidal electrolytes. *J. Coll. Sci. Imp. U. Tok.* **1964**, *19*, 722–728.

[26] Wang, H.; Zhou, W.; Ho, D. L.; Winey, K. I.; Fischer, J. E.; Glinka, C. J.; Hobbie, E. K. Dispersing single-walled carbon nanotubes with surfactants: A small angle neutron scattering study. *Nano Lett.* **2004**, *4*, 1789–1793.

[27] McDonald, T. J.; Engtrakul, C.; Jones, M.; Rumbles, G.; Heben, M. J. Kinetics of PL quenching during single-walled carbon nanotube rebundling and diameter-dependent surfactant interactions. *J. Phys. Chem. B* **2006**, *110*, 25339–25346.

[28] Nair, N.; Kim, W. J.; Braatz, R. D.; Strano, M. S. Dynamics of surfactant-suspended single-walled carbon nanotubes in a centrifugal field. *Langmuir* **2008**, *24*, 1790–1795.